HORIBA

Raman

How Raman Spectroscopy can measure nanoelectronics structures

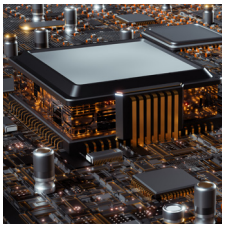

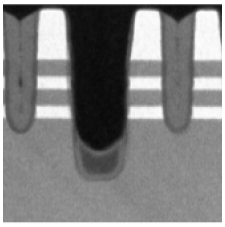

Application Note

Semiconductors
RA102

T. Nuytten[1], J. Bogdanowicz[1], S. Sergeant[1], C. Fleischmann[1,2], Agnès Tempez[3], Ophélie Lancry[3], Marc Chaigneau[3]

[1]IMEC, Kapeldreef 75, B-3001 Leuven, Belgium, [2]KU Leuven, Department of Physics and Astronomy, Quantum Solid-State Physics, Celestijnenlaan 200D, B-3001 Leuven, Belgium, [3]HORIBA FRANCE SAS, Palaiseau, France

Abstract: Raman spectroscopy is a powerful tool for analyzing semiconductor materials because it's non-destructive, non-contact, fast, and it can measure numerous properties. However, as semiconductor devices get smaller, the technique faces a spatial resolution challenge due to its inherent optical limitations. To overcome this, a group @ imec has developed a method based on polarization-induced enhancement allowing to effectively detect structures much smaller than the light's wavelength. As a result, Raman spectroscopy can now measure things like stress and composition at the nanoscale, which was previously difficult. Moreover, this method examines the entire material structure, not just the surface, turning Raman spectroscopy into a tool that can measure both the volume and shape of materials. This opens up new possibilities for Raman spectroscopy to be used in the fab environment.

Keywords: Raman spectroscopy, semiconductors, dimensional metrology, SiGe, cavity depth, GAA-FET, 3DNAND, memories

Introduction

Raman spectroscopy is an essential tool for the characterization of semiconductors as it provides non-destructive, high-throughput, and versatile measurements of various material properties, including stress, composition, and crystalline structure. However, Raman spectroscopy's spatial resolution is limited by the diffraction limit to about 200-300 nanometers, which can be insufficient for analyzing the increasingly smaller features of modern electronic devices. This application note aims at showing how it is possible to make use of the resonant coupling phenomenon when the light polarization is aligned with device structures with dimensions much smaller than the incident wavelength [1-6]. This polarization-induced enhancement allows Raman microscopy to reach nanoscale information without hardware modifications of the instrumentation. The nanofocusing mode is achievable by selecting the appropriate arrangement of incident polarization and structure angular orientation. In addition, since the nanofocusing effect is highly dependent on the dimensions of the nanostructure, this phenomenon can also be used to study the dimensions themselves, which is a crucial aspect of semiconductor metrology. The intensity of the obtained signals scales directly with the probed volume at the nanoscale. Nanometer-level sensitivity to dimensions such as the width of semiconductor and metal lines has been shown.

Experimental and Results

The data shown in this note were obtained using a HORIBA LabRAM HR spectrometer equipped with 405, 532, 633, and 785 nm excitation lasers in backscattering geometry. In this note, the 405 nm laser was used for excitation, which, thanks to the penetration depth of only ~140 nm in Si, has the highest surface sensitivity. The other acquisition parameters were (i) 60 s integration time, (ii) 1800 or 2400 gr/mm gratings, (iii) 100× 0.9NA objective, resulting in a spot size slightly below 1 µm, and (iv) 160 kW/cm^2 laser power density to limit heating-induced peak shifts (<1 cm^{-1} is acceptable when mainly relative peak intensities are considered). The polarization from the linearly polarized, solid-state laser source was adjusted using a k/2 waveplate followed by a polarizer optic (linear polarizer) for precise control of the incident polarization, which is critical in these experiments.

To illustrate the nano-focusing effect, Fig. 1 shows the Raman spectrum of a 100 nm wide fin consisting of an alternating stack of $Si_{75}Ge_{25}$ and Si layers, grown on Si substrate, with a pitch of 420 nm. The incident parallel polarization to the fin results in Si–Si scattering contributions from the SiGe layers and Si layers/Si substrate at 520 cm^{-1} that are well separated in the Raman spectrum.

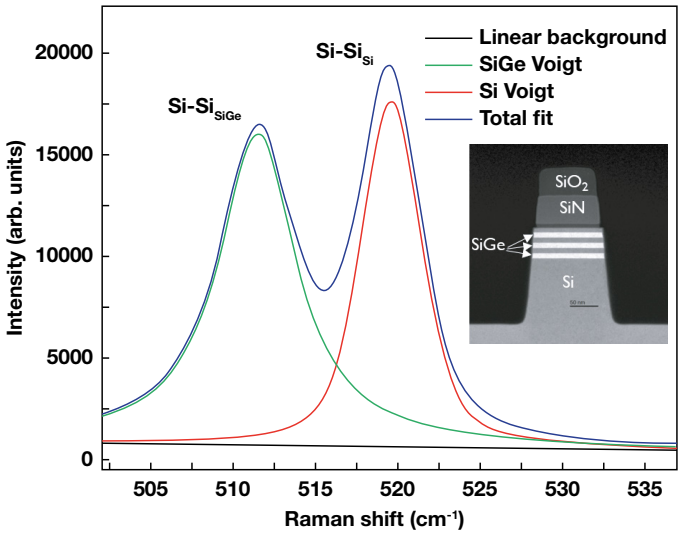

Figure 1: High spectral resolution Raman spectrum of a stacked semiconductor device containing alternating Si and $Si_{75}Ge_{25}$ layers. Both Si- and SiGe-related Si–Si vibrations can be deconvoluted and considered distinctively. The inset shows a cross-section profile of the structure obtained by high-angle annular dark-field scanning tunneling electron microscopy (HAADF STEM), where the alternating stack of SiGe and Si layers is visible.

Now, we will show three examples to prove the potential of this nano-focusing effect: (i) determination of the cavity depth in gate-all-around field effect transistors, (ii) determination of the cavity depth in 3D memory, and (iii) characterization of the critical dimension of TiN metal lines. In gate-all-around field-effect transistors, a metrology challenge arises when the SiGe in the Si/SiGe stack is selectively etched from the sides, exposing the Si transistor channel for further processing (see Fig. 2). The depth of this cavity is a critical parameter to control, but it is difficult to measure using standard profilometric techniques or most top-down methods, such as critical dimension-scanning electron microscopy. Three samples prepared with three different etching times have been measured. The graph in Fig. 3 plotting the SiGe Raman signal normalized to the Si signal coming from the Si substrate and the remaining Si channel versus the cavity depth as measured by transmission electron microscopy (TEM) shows a linear decrease. Fig. 3 also shows that the normalized SiGe Raman intensity follows the ratio of the normalized remaining SiGe volume (V/V_0 as determined by TEM) represented as a dash line. The Raman measurement is as sensitive as the true volumetric measurement realized by TEM.

In 3D memory structures, the same cavity depth determination issue arises upon etching the polysilicon cavity. Fig. 4 shows spectra normalized to the crystalline silicon peak featuring the decrease of the polysilicon contribution (broader peak at 5 cm^{-1} lower wavenumber than crystalline silicon) as the cavity is being etched. The ratio between this intensity and the cSi background serves as a quantitative indicator of the remaining PolySi volume, and consequently, the depth of the cavity. TEM measurements have confirmed a direct one-to-one correlation between the normalized PolySi Raman intensity and the etched cavity depth (not shown).

The third example deals with TiN lines of varying critical dimensions (Fig. 5) and demonstrates that the method can also be applied to non-Raman active materials. To do that, the incident polarization needs to be perpendicular to the metal lines (Fig. 5) such that now the excitation light is confined into the region in between the lines, which is filled with SiO_2. This enables the light to reach the underlying Si substrate and the substrate Raman intensity will depend on the critical dimension (CD) of the metal lines it has gone through. Fig. 6 depicts the linear relationship between the normalized Si signal (to pure Si, CD=0) with increasing the critical dimension. The Si Raman response has been measured using three excitation wavelengths and Fig. 6 shows that the highest sensitivity is reached with the 785 nm longest wavelength. This comes from the effective extinction coefficient κ_eff which in these systems increases with increasing wavelength. This coefficient reflects the light transmission and the returning Si Raman signal through the metal grating in the photonic crystal.

The power of the nanofocusing effect has been further demonstrated using forksheet transistor architectures after replacement gate processing, comprising two gratings of first the n and p metal-oxide-semiconductor (MOS) transistor structures and then subsequently 150–200 nm-

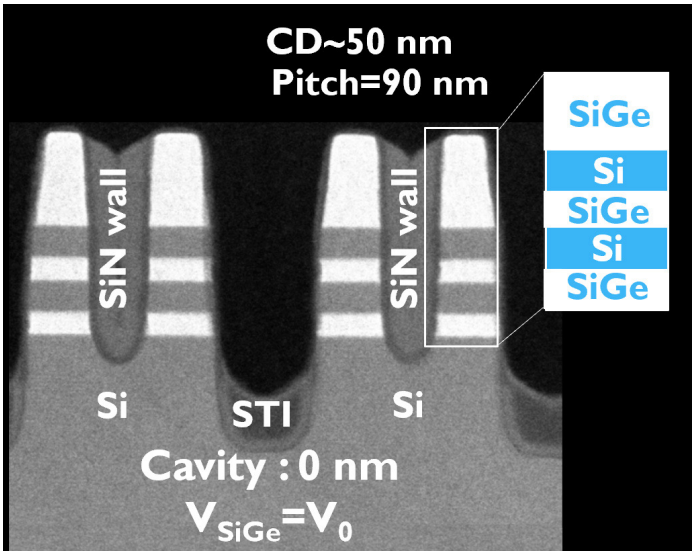

Figure 2: TEM micrograph of the unetched gate-all-around field-effect transistors structure where the alternating stack of SiGe and Si layers is visible.

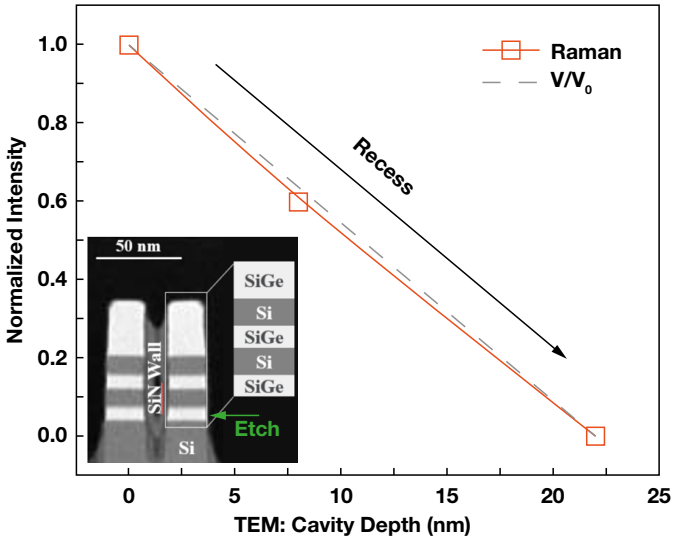

Figure 3: (a) Normalized integrated intensity of the Si–Si vibration coming from $Si_{75}Ge_{25}$ to the Si–Si vibration coming from Si, as a function of the cavity depth as determined by TEM. As the etch cavity gets larger (see green arrow in the TEM micrograph of the unetched structure), the profile follows the nominal remaining volume of SiGe (V/V0, dashed line).

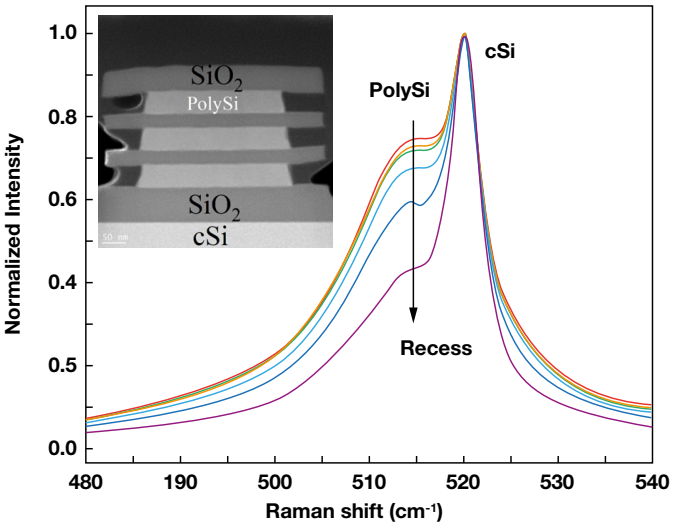

Figure 4: Set of spectra acquired from samples with increasing PolySi etch quantities displayed normalized to the Si background. We can clearly see the reduced PolySi shoulder upon with increasing etch. The inset shows a HAADF STEM image of the structure under study with alternating PolySi and SiO_2 layers.

thick amorphous Si (aSi) lines, with both gratings orthogonal to each other. The transistor structures are composed of alternating layers of Si and $Si_{75}Ge_{25}$ progressively etched away from between the Si layers. Fig.7 (a) and (b) show the Raman response when the incident laser is polarized parallel to the fin and rotated by 90° (then aligned with aSi lines), respectively. In the conditions of polarization parallel to the fin, the SiGe contribution seen as a shoulder on the cSi peak and as a peak from the Si-Ge scattering goes down upon etching while no signal from aSi is detected. Upon 90° rotation of the incident polarization, we can observe complete extinction of the cSi and SiGe contributions and the presence of aSi peak at 480 cm^{-1} with an intensity which remains unchanged upon the etching step.

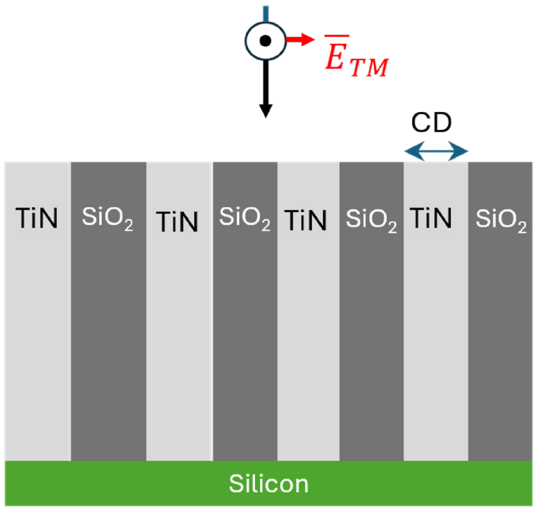

Figure 5: Schematic diagram of the TiN lines grating with SiO_2 spacing.

This "ON/OFF" effect requires a strict and precise control of the polarization, realized using a first k/2 waveplate to rotate the incident polarization, followed by a linear polarizer optic still in the incident path, to further purify the incident polarization selection. Thanks to precise polarization control, simply rotating the incident polarization enables full selectivity between the two independent gratings. This, in turn, allows Raman analysis—such as mechanical stress, composition, and doping—to be applied individually to each grating.

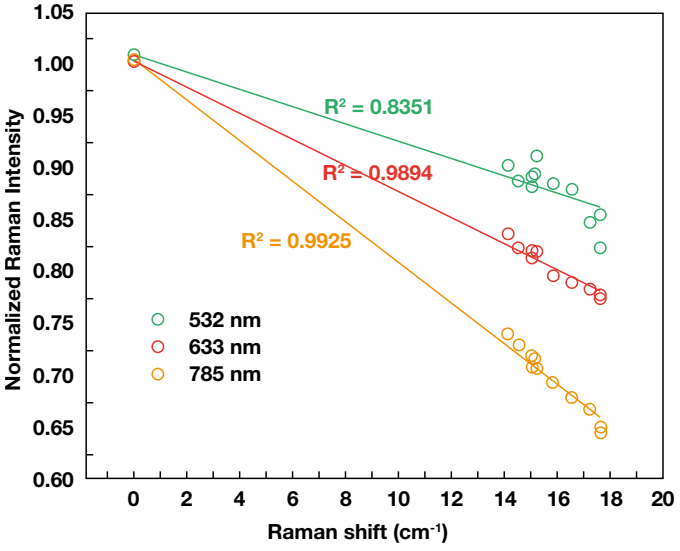

Figure 6: Normalized Raman intensity from a TiN grating with underlying Si as a function of the TiN linewidth as measured by CD-SEM. The technique can detect tiny variations in critical dimension (CD) with a sensitivity that improves as the wavelength of the probing laser increases.

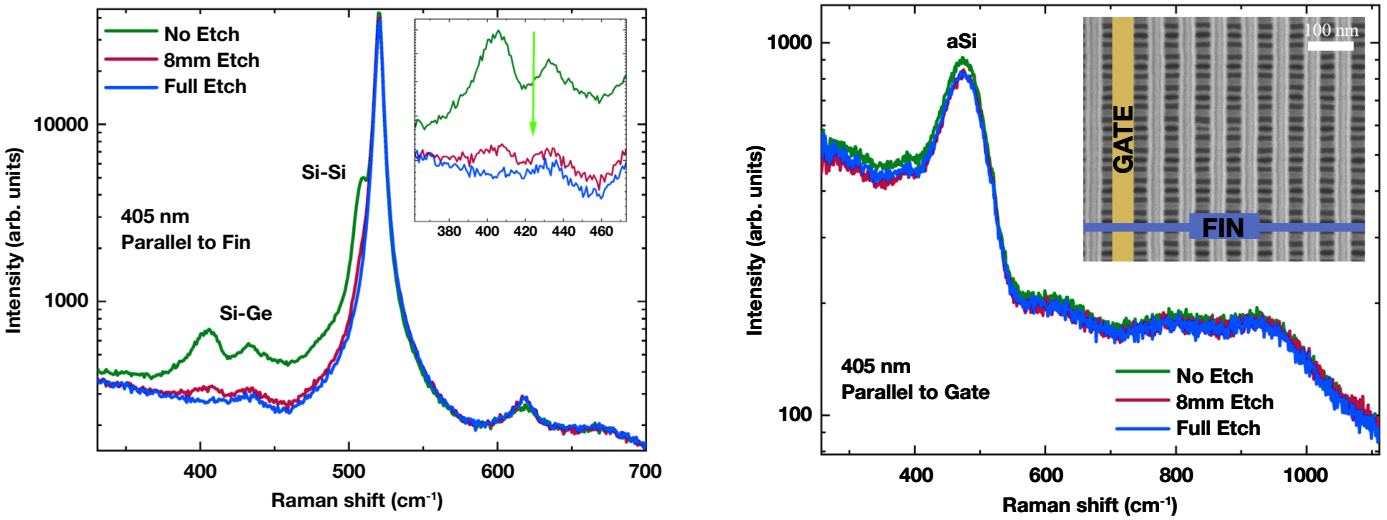

Figure 7: (a) Raman spectra with polarization parallel to the fin structures. A strong sensitivity to remaining $Si_{75}Ge_{25}$ content is observed, and no aSi material from the dummy gate is detected. (b) Raman spectra recorded with polarization parallel to the gate. Only the aSi is observed in the spectra, and since this material is not subject to the etch process, the intensity is unaffected. The inset shows a top-down SEM image of the structures under investigation with gate and fin directions indicated.

Table 1: List of studied cases/devices applications of Raman nanofocusing effect detailing materials involved, dimension conditions, information of interest, and Raman signal to monitor for each application.

Devices	Materials	CD min	Information	Raman measurement
Fin-FET 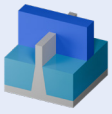	Strained Germanium lines / SiGe lines separated by SiO_2	20 nm	Average stress	Separate TO/LO excitation for anisotropic average stress
			Average Ge%	Ge-Ge to Si-Ge peak ration
Nanosheets and forksheets gate-all-around transistors 	SiGe/Si alternating stack Study of SiGe etching process to leave Si transistor channel	50 nm	Cavity depth	Si-Si in SiGe (510 cm^{-1}) peak intensity normalized to Si-Si peak intensity (521 cm^{-1})
3D flash memories 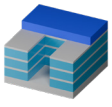	Polysilicon: Study of 50 nm thick polysilicon layers stacked between 30 nm thick SiO_2 layers		Cavity depth/wafer mapping	Normalized Poly (510 cm^{-1}) peak intensity to Si-Si peak intensity (521 cm^{-1})
Interconnects 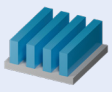	W and TiN lines separated by SiO_2 on Si	<20 nm	CD	Transmission: Normalized Si peak intensity Better sensitivity with 785 nm laser

Conclusions and perspectives

In conclusion, this note describes the method allowing Raman microscopy to characterize nanosized advanced electronic structures. When the incident light is polarized parallel to the fin edges and the fin width is only a small fraction of the incident wavelength, cavity depth information is accessible from looking at the SiGe normalized intensity. When the incident light is polarized orthogonal to the grating metal lines, critical dimension is at reach when monitoring normalized silicon response. Raman spectroscopy becomes thus a dimensional metrology tool for industry-relevant structures. Other device application examples are given in Table 1 together with materials involved, dimension conditions, information of interest, and Raman signal to monitor. Combined with the wide range of applications at the nanometer scale, this makes it an essential toolkit in semiconductor manufacturing. We expect these developments to see increasing use in high-volume manufacturing as 300 mm-capable Raman and photoluminescence (PL) tools are being introduced into semiconductor fabrication facilities.

References

1. T. Nuytten, J. Bogdanowicz, S. Sergeant, C. Fleischmann, Appl. Phys. Lett. 125, 053506 (2024), https://doi.org/10.1063/5.0219438.
2. Thomas Nuytten, Janusz Bogdanowicz. (2021), Method and apparatus for measuring a lateral depth in a microstructure. Patent US12216057B2. USA.
3. T. Nuytten, J. Bogdanowicz, L. Witters, G. Eneman, T. Hantschel, A. Schulze, P. Favia, H. Bender, I. De Wolf, W. Vandervorst, APL Mater. 6, 058501 (2018). https://doi.org/10.1063/1.4999277
4. J. Bogdanowicz, T. Nuytten, A. Gawlik, A. Schulze, I. De Wolf, W. Vandervorst; Appl. Phys. Lett. 22; 108 (8): 083106 (2016). https://doi.org/10.1063/1.4942603
5. Janusz Bogdanowicz, Thomas Nuytten, Andrzej Gawlik, Stefanie Sergeant, Yusuke Oniki, Pallavi Puttarame Gowda, Hans Mertens, and Anne-Laure Charley, Nano Letters 24 (4), 1191 (2024). DOI: 10.1021/acs.nanolett.3c04033
6. T. Nuytten, T. Hantschel, D. Kosemura, A. Schulze, I. De Wolf, W. Vandervorst; Edge-enhanced Raman scattering in narrow sGe fin field-effect transistor channels. Appl. Phys. Lett.; 106 (3), 033107 (2015). https://doi.org/10.1063/1.4906537
7. A. Gawlik, J. Bogdanowicz, T. Nuytten, A.-L. Charley, L. Teugels, J. Misiewicz, W. Vandervorst; Critical dimension metrology using Raman spectroscopy. Appl. Phys. Lett.; 117 (4): 043102 (2020). https://doi.org/10.1063/5.0013506

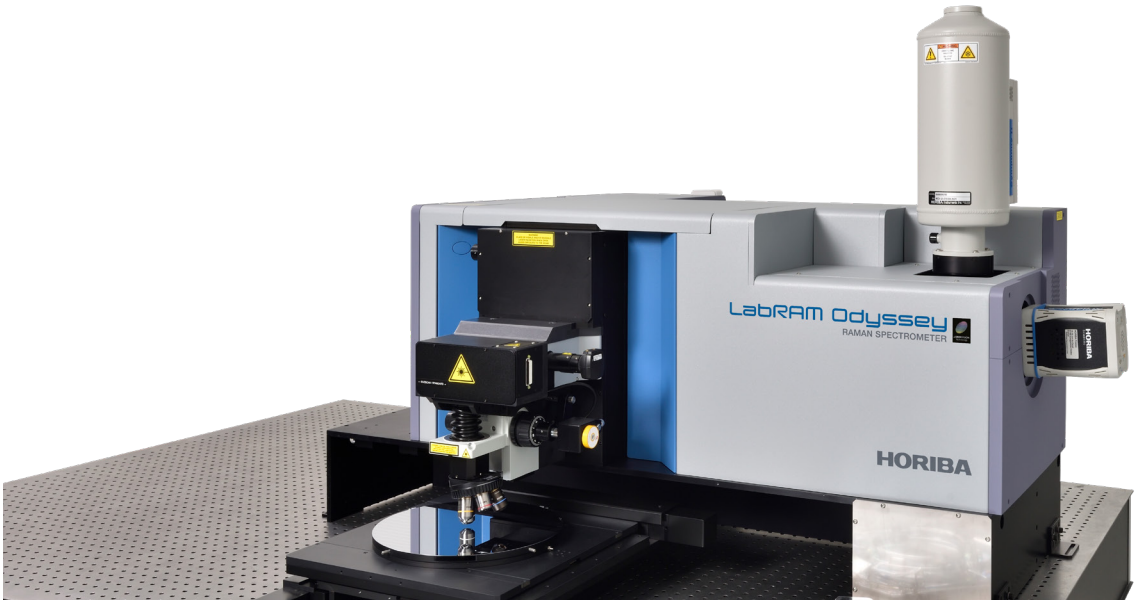

Figure 8: LabRAM Odyssey Semiconductor

info.sci@horiba.com **www.horiba.com/scientific**

USA:	+1 732 494 8660	**Italy:**	+39 06 51 59 22 1	**Singapore:**	+65 (6) 745-8300
France:	+33 (0)1 69 74 72 00	**Japan:**	+81(75)313-8121	**Taiwan:**	+886 3 5600606
Germany:	+49 (0) 6172 1396 0	**China:**	+86 (0)21 6289 6060	**Brazil:**	+55 (0)11 2923 5400
UK:	+44 (0)1604 542 500	**India:**	+91 (80) 4127 3637	**Other:**	+33 (0)1 69 74 72 00